
中国物理 **B**
**Chinese
Physics B**

Volume 22 Number 10 October 2013

Formerly *Chinese Physics*

A Series Journal of the Chinese Physical Society
Distributed by IOP Publishing

Online: iopscience.iop.org/cpb
cpb.iphy.ac.cn

CHINESE PHYSICAL SOCIETY
IOP Publishing

Chinese Physics B (First published in 1992)

Published monthly in hard copy by the Chinese Physical Society and online by IOP Publishing, Temple Circus, Temple Way, Bristol BS1 6HG, UK

Institutional subscription information: 2013 volume

For all countries, except the United States, Canada and Central and South America, the subscription rate is £977 per annual volume.

Single-issue price £97. Delivery is by air-speeded mail from the United Kingdom.

Orders to:

Journals Subscription Fulfilment, IOP Publishing, Temple Circus, Temple Way, Bristol BS1 6HG, UK

For the United States, Canada and Central and South America, the subscription rate is US\$1930 per annual volume. Single-issue price US\$194. Delivery is by transatlantic airfreight and onward mailing.

Orders to:

IOP Publishing, PO Box 320, Congers, NY 10920-0320, USA

© 2013 Chinese Physical Society and IOP Publishing Ltd

All rights reserved. No part of this publication may be reproduced, stored in a retrieval system, or transmitted in any form or by any means, electronic, mechanical, photocopying, recording or otherwise, without the prior written permission of the copyright owner.

Supported by the National Natural Science Foundation of China, the China Association for Science and Technology, and the Science Publication Foundation, Chinese Academy of Sciences

Editorial Office: Institute of Physics, Chinese Academy of Sciences, PO Box 603, Beijing 100190, China

Tel: (86-10) 82649026 or 82649519, Fax: (86-10) 82649027, E-mail: cpb@aphy.iphy.ac.cn

主管单位: 中国科学院

国内统一刊号: CN 11-5639/O4

主办单位: 中国物理学会和中国科学院物理研究所

广告经营许可证: 京海工商广字第0335号

承办单位: 中国科学院物理研究所

编辑部地址: 北京 中关村 中国科学院物理研究所内

主 编: 欧阳钟灿

通 讯 地 址: 100190 北京 603 信箱

出 版: 中国物理学会

Chinese Physics B 编辑部

印刷装订: 北京科信印刷厂

电 话: (010) 82649026, 82649519

编 辑: Chinese Physics B 编辑部

传 真: (010) 82649027

国内发行: Chinese Physics B 出版发行部

E-mail: cpb@aphy.iphy.ac.cn

国外发行: IOP Publishing Ltd

“Chinese Physics B”网址:

发行范围: 公开发行

<http://cpb.iphy.ac.cn>(编辑部)

国际统一刊号: ISSN 1674-1056

<http://iopscience.iop.org/cpb> (IOP)

Published by the Chinese Physical Society

顾问 Advisory Board

陈佳洱 教授, 院士
北京大学物理学院, 北京 100871

Prof. Academician Chen Jia-Er
School of Physics, Peking University, Beijing 100871, China

冯 端 教授, 院士
南京大学物理系, 南京 210093

Prof. Academician Feng Duan
Department of Physics, Nanjing University, Nanjing 210093, China

黄祖洽 教授, 院士
北京师范大学低能核物理研究所,
北京 100875

Prof. Academician Huang Zu-Qia
Institute of Low Energy Nuclear Physics, Beijing Normal University, Beijing
100875, China

李政道 教授, 院士

Prof. Academician T. D. Lee
Department of Physics, Columbia University, New York, NY 10027, USA

李荫远 研究员, 院士
中国科学院物理研究所, 北京 100190

Prof. Academician Li Yin-Yuan
Institute of Physics, Chinese Academy of Sciences, Beijing 100190, China

丁肇中 教授, 院士

Prof. Academician Samuel C. C. Ting
LEP3, CERN, CH-1211, Geneva 23, Switzerland

杨振宁 教授, 院士

Prof. Academician C. N. Yang
Institute for Theoretical Physics, State University of New York, USA

杨福家 教授, 院士
复旦大学物理二系, 上海 200433

Prof. Academician Yang Fu-Jia
Department of Nuclear Physics, Fudan University, Shanghai 200433, China

周光召 研究员, 院士
中国科学技术协会, 北京 100863

Prof. Academician Zhou Guang-Zhao (Chou Kuang-Chao)
China Association for Science and Technology, Beijing 100863, China

王乃彦 研究员, 院士
中国原子能科学研究院, 北京 102413

Prof. Academician Wang Nai-Yan
China Institute of Atomic Energy, Beijing 102413, China

梁敬魁 研究员, 院士
中国科学院物理研究所, 北京 100190

Prof. Academician Liang Jing-Kui
Institute of Physics, Chinese Academy of Sciences, Beijing 100190, China

(Continued)

Bipolar resistive switching in $\text{BiFe}_{0.95}\text{Zn}_{0.05}\text{O}_3$ films*

Yuan Xue-Yong(袁学勇)^{a)}, Luo Li-Rong(罗丽荣)^{b)}, Wu Di(吴迪)^{c)}, and Xu Qing-Yu(徐庆宇)^{a)†}

^{a)}Department of Physics, Southeast University, Nanjing 211189, and Key Laboratory of MEMS of the Ministry of Education, Southeast University, Nanjing 210096, China

^{b)}School of Materials Science and Technology, Nanjing University of Aeronautics and Astronautics, Nanjing 210016, China

^{c)}Department of Materials Science and Engineering, Nanjing University, Nanjing 210008, China

(Received 30 March 2013; revised manuscript received 10 May 2013)

Bipolar resistive switching is studied in $\text{BiFe}_{0.95}\text{Zn}_{0.05}\text{O}_3$ films prepared by pulsed laser deposition on (001) SrTiO_3 substrate, with LaNiO_3 as the bottom electrode, and Pt as the top electrode. Multiple steps of resistance change are observed in the resistive switching process with a slow voltage sweep, indicating the formation/rupture of multiple conductive filaments. A resistive ratio of the high resistance state (HRS) to the low resistance state (LRS) of over three orders of magnitude is observed. Furthermore, the conduction mechanism is confirmed to be space-charge-limited conduction with the Schottky emission at the interface with the top Pt electrodes in the HRS, and Ohmic in the LRS. Impedance spectroscopy demonstrates a conductive ferroelectric/interfacial dielectric 2-layer structure, and the formation/rupture of the conductive filaments mainly occurs at the interfacial dielectric layer close to the top Pt electrodes.

Keywords: multiferroics, resistive switching

PACS: 77.55.Nv, 72.20.Ht, 73.50.Fq

DOI: 10.1088/1674-1056/22/10/107702

1. Introduction

Resistance random access memory (RRAM)^[1,2] based on resistive switching (RS) is deemed to be the most promising category of next-generation nonvolatile memory and has attracted much interest recently due to its simple structure, rapid write/erase operation, low power consumption, and high-density integration.^[3-5] Furthermore, RS is widely observed in transition metal oxides and perovskite oxides, such as NiO ,^[6] TiO_2 ,^[7] $(\text{PrCa})\text{MnO}_3$,^[8] and SrTiO_3 .^[9] Although RS phenomena have been studied for decades, the mechanism is still not clearly identified. Various mechanisms have been proposed to explain the reversible switching of resistance state, including formation/rupture of conductive filaments,^[10,11] Schottky barriers at interfaces,^[12,13] etc.

As the only single phase multiferroic material above room temperature, BiFeO_3 (BFO) has attracted great attention due to its potential application in spintronics, photoelectronics.^[14-16] The RS effect was first observed by Yang in Ca-doped BiFeO_3 epitaxial film,^[17] and later was also observed in BiFeO_3 films, and different models have been applied to explain the physical origin of this behavior. Bipolar resistive switching (BRS) has been observed by Shuai, which he attributed to the electric field-induced carrier trapping and detrapping.^[18] Li attributed the BRS to the formation/rupture of the nanoscale metal filaments due to the diffusion of the top electrodes under the bias voltage.^[19] Yin attributed the BRS to the formation/rupture

of the conductive paths formed by the oxygen vacancies.^[20] Wang reported large ferroelectric resistive switching and the observation that the forward direction of rectifying current can be reversed by polarization — this was explained by the polarization-modulated Schottky-like barriers.^[21] In this paper, we report the BRS in $\text{BiFe}_{0.95}\text{Zn}_{0.05}\text{O}_3$ (BFZO) films, and impedance spectroscopy has been employed to understand the BRS mechanism.

2. Experimental details

BFZO films were prepared by pulsed laser deposition (PLD) with a ceramic target $\text{Bi}_{1.05}\text{Fe}_{0.95}\text{Zn}_{0.05}\text{O}_3$ (5% excess Bi was introduced to compensate for volatile loss). Zn was incorporated to decrease the leakage current.^[22,23] The detailed preparation process has been described before.^[24,25] As the bottom electrode and buffer layer, an LaNiO_3 (LNO) (30-nm thick) was first deposited on (001) SrTiO_3 (STO) substrate at 850 °C under oxygen pressure of 20 Pa. Then the BFZO film (about 80 nm) was deposited at 700 °C under oxygen pressure of 2 Pa. After deposition, the heterostructure was annealed at 550 °C for 30 minutes and then cooled down to room temperature in an oxygen pressure of 1×10^5 Pa. Round Pt top electrodes of 100- μm diameter were deposited on the films through a shadow mask. The structure of the film was examined by X-ray diffraction (XRD, Rigaku SmartLab3) with $\text{Cu K}\alpha$ radiation. The electrical measurements were carried out

*Project supported by the National Natural Science Foundation of China (Grant No. 51172044), the Natural Science Foundation of Jiangsu Province of China (Grant No. BK2011617), the National Key Project for Basic Research of China (Grant No. 2010CB923404), the 333 Project of Jiangsu Province, by NCET-09-0296, the Scientific Research Foundation for Returned Overseas Chinese Scholars, the State Education Ministry, and Southeast University (Grant No. Seu201106).

†Corresponding author. E-mail: xuqingyu@seu.edu.cn

© 2013 Chinese Physical Society and IOP Publishing Ltd

<http://iopscience.iop.org/cpb> <http://cpb.iphy.ac.cn>

using a Keithley 2400 SourceMeter and 2182A NanovoltMeter at room temperature. During the measurements, the bias is defined as positive when the current flows from the LNO bottom electrode to the Pt top electrode. Complex impedance measurements were performed in the frequency range from 40 Hz to 110 MHz at room temperature using an impedance analyzer (Agilent 4294A).

3. Results and discussion

The XRD pattern of BFZO film is shown in Fig. 1. All the peaks can be indexed to a pseudo-cubic structure with only (00*n*) peaks observed, which demonstrates a highly preferred orientation of BFZO film along the *c* axis. The small diffraction peak marked by an asterisk is from the STO substrate. The (00*n*) peaks of STO and LNO are located at the right of BFZO, for they have smaller pseudo-cubic *c* lattice constants (BFO: 3.96 Å,^[26] STO: 3.91 Å,^[27] LNO: 3.84 Å^[28]).

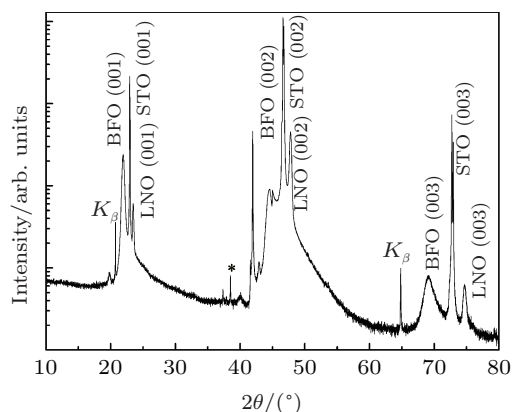


Fig. 1. XRD patterns of STO/LNO/BFZO.

Figure 2(a) shows the *I*–*V* curves obtained under dc voltage sweep mode with 30 mV/step. The schematic diagram of the STO/LNO/BFZO/Pt device structure is illustrated in the left bottom inset of Fig. 2(a). As shown in Fig. 2(a), the forming was achieved at a voltage of 2.31 V. After the initial forming process, a typical BRS can be observed in the BFZO film. When a positive voltage is applied on the LNO bottom electrode, the resistance shows an abrupt decrease from the high resistance state (HRS) to the low resistance state (LRS) (defined as SET process) at 1.62 V, and the current becomes nearly two orders of magnitude larger, protected by the 1 mA compliance current. When negative voltage is applied, the resistance switches back from LRS to HRS at –1.16 V (defined as RESET process). As illustrated in the picture, the electric currents in the HRS in the following SET processes are much larger than those in the forming process and the switching voltages in the SET processes are lower than those in the forming process. (We repeated measurements of the *I*–*V* curves under the same conditions another 10 times, and the

SET voltage was never more than 1.92 V.) The electroforming process generates defects inside the BFZO layer, mostly by the thermally assisted electromigration of oxygen ions.^[29] According to the filament model,^[30,31] the oxygen vacancies are aligned to form tiny conductive filaments under the electric field, leading to the transition to the LRS during the forming process. Even when the LRS is transformed to the HRS, fragmented or disconnected filaments exist in the BFZO film due to the limited migration of the oxygen ions in the film; consequently the resistance of the HRS of the devices is always much lower than that of the as-made cells.^[29] Furthermore, the RESET process is not as rapid as the SET process — it shows gradual change with multiple steps. We measured the *I*–*V* hysteresis curves several times to check the reproducibility. Similar multistep switching behavior has been observed in the RRAM devices and was explained by the formation of multiple conductive filaments.^[32,33] We also performed statistics of SET/RESET voltage with different cells (not shown here). Our device shows stable resistive switching behavior, the SET voltage was from 1.16 V to 2.02 V and RESET voltage varied

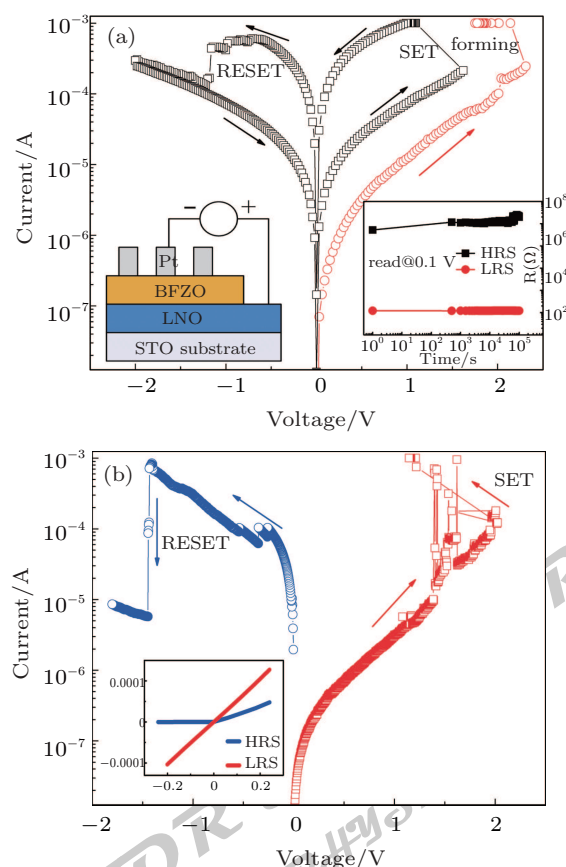


Fig. 2. (color online) (a) The typical *I*–*V* characteristics of the LNO/BFZO/Pt structure using a voltage sweeping rate of 30 mV/step. Left bottom inset shows the schematic device structure; right bottom inset shows retention of the HRS and LRS with reading voltage of 0.1 V. (b) *I*–*V* characteristics using a voltage sweeping rate of 3 mV/step. Inset is the *I*–*V* curves with voltage sweeping from –0.2 V to +0.2 V.

from -1.04 V to -1.60 V. The retention property of our device measured with 0.1 V at room temperature is shown in the right bottom inset of Fig. 2(a). As can be seen, up to 10^5 s, resistance in both the HRS and LRS shows little deterioration and the resistance ratio of HRS/LRS is around 10^3 without degradation.

In order to explore the underlying physics in our device further, we used the dc voltage sweep mode with 3 mV/step, and the I - V curves are shown in Fig. 2(b). Interestingly, this time the SET process also shows a stepwise switching phenomenon, the SET and RESET voltage were 2.00 V and -1.43 V, respectively. An I - V sweep between -0.2 V and $+0.2$ V was performed in the LRS and HRS, as shown in the inset of Fig. 2(b). Clear rectifying characteristics were observed in the HRS, suggesting the formation of a Schottky barrier. Generally, the rectifying behavior comes from a p-n junction or a metal-semiconductor Schottky-like junction due to the energy barrier at the interface. The work function of LNO is 4.5 eV,^[34] Pt is 5.3 eV, and BFO can be taken as 4.7 eV.^[35] In addition, the BFZO/LNO interface is an epitaxial contact, whereas the Pt/BFO interface is a nonepitaxial contact. The interfacial layer formed at the nonepitaxial Pt/BFO interface may be much thicker than the one formed at the epitaxial BFO/LNO interface, which shows a larger contact resistance. Therefore, a Schottky junction is more likely to be formed at the Pt/BFZO interface; this has been confirmed experimentally by Tsurumaki.^[36]

Figures 3(a) and 3(b) show the I - V curve in the positive and negative voltage regions, which are plotted in log-log scale. As illustrated in the figure, it is clear that the slope of LRS and HRS in low field is close to 1, which can be attributed to Ohmic behavior. As for the high electric field in HRS, it is a bit more complicated to determine the conduction mechanism. The classical nonlinear conduction mechanisms for BiFeO₃ mainly include space-charge-limited conduction (SCLC), Schottky emission, and Poole-Frenkel (PF) emission.^[37] The current density for SCLC can be expressed as^[37,38]

$$J_{\text{SCLC}} = \frac{9\mu\epsilon_0 K V^2}{8 d^3}, \quad (1)$$

where μ represents the carrier mobility. According to Eq. (1), the plots of $\log(I)$ versus $\log(V)$ should show a linear behavior with a slope of 2. As shown in Figs. 3(a) and 3(b), the slopes in high electric field are 1.88 and 1.76, respectively. This suggests the dominant conduction mechanism in the high voltage region is SCLC. However, the slight deviation of the slope from 2 might be due to deep-level traps,^[39,40] and there is contribution from another conduction mechanism.

The Schottky barrier has been confirmed by the rectifying I - V curve in the HRS. For the Schottky emission, which arises from a difference in Fermi level between metal and semiconductor, the current density is^[37]

$$J_s = AT^2 \exp\left[-\frac{\phi}{k_B T} - \frac{1}{k_B T} \left(\frac{q^3 U}{4\pi\epsilon_0 K d}\right)^{1/2}\right], \quad (2)$$

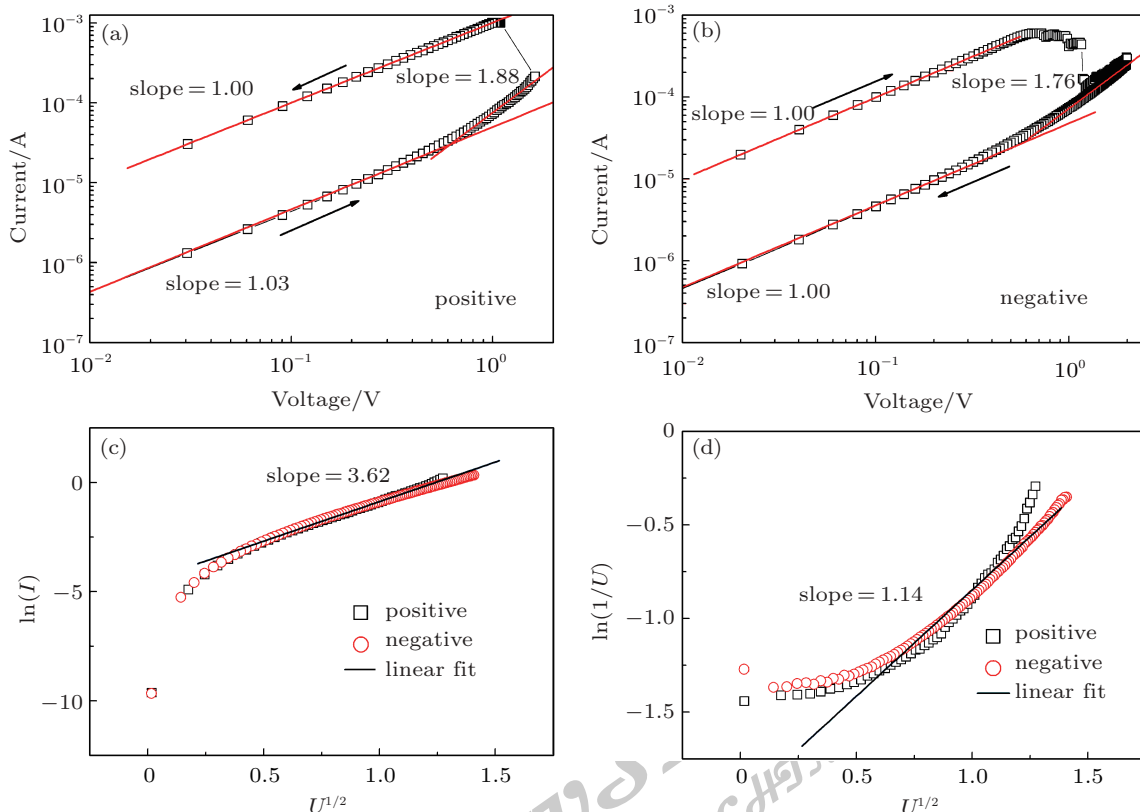


Fig. 3. (color online) Typical I - V characteristics in log-log scale of the LNO/BFZO/Pt structure with (a) positive voltage and (b) negative voltage, respectively. The I - V data in the HRS are fitted by (c) Schottky emission and (d) PF emission, respectively.

where ϕ is the height of Schottky barrier and K is the dielectric constant of the film. The third mechanism is PF emission, which is considered to be a common leakage mechanism in BFO film.^[37,41] The bulk-limited PF emission involves the consecutive hopping of charges between defect trap centers. The conductivity for PF emission obeys^[37,42]

$$\frac{I}{U} = \frac{J}{E} = \sigma_{\text{PF}} = c \exp \left[\frac{E_1}{k_{\text{B}}T} - \frac{1}{k_{\text{B}}T} \left(\frac{q^3 U}{\pi \epsilon_0 K d} \right)^{1/2} \right], \quad (3)$$

where c is a constant; E_1 is the trap ionization energy; k_{B} is the Boltzmann constant. The rather poor linear fit of $\log(I/U)$ versus $U^{1/2}$ [Fig. 3(d)] excludes the PF conduction mechanism. Quite good linear fitting of $\log(I)$ versus $U^{1/2}$ has been obtained at high field [Fig. 3(c)]; a dielectric constant of ~ 3.62 was obtained, which is comparable to the reported dielectric constant of 6.25 from the index of refraction of 2.5 for BiFeO₃ by Iakovlev *et al.*^[43] Therefore, the Schottky emission also has contribution in the HRS state. As a result, conductive filaments and the Schottky barrier exist simultaneously during the resistive switching process.

In order to further study the origin of the resistive switching, we measured the impedance spectra after the forming process on different cells at room temperature. Figure 4 shows the impedance data of the HRS and LRS on log-scale in Cole–Cole form. It is obvious to see that the impedance spectrum of HRS consists of two semi-circles while only one semi-circle exists in that of LRS. The two semi-circles are attributed to film and interface contributions and usually fitted using RC elements.^[44] In this regard, the resistance transition from HRS to LRS can be attributed to a broken Schottky barrier in the interface. The impedance spectra of HRS and LRS are fitted using the conventional RC elements with the equivalent circuits, as shown in Fig. 4. The RC elements correspond to charge transport either internal to the film or through the film interface. R_0 represents all the Ohmic resistance including wires for the measurement. The obtained parameters are summarized in Table 1. By assuming the parallel RC elements, the calculated data are in good agreement with the experimental impedance spectra. Note that the cells in the HRS and LRS measurements are not the same cell. It can be seen that the calculated R_1 , C_1 , and R_0 in HRS and LRS are similar. Combined with the I – V and impedance measurements, it can be seen that a high resistive layer emerges at the interface with the top Pt layer in the HRS.

Table 1. Summary of the equivalent circuit parameters by fitting the impedance spectra in the HRS and LRS.

Resistance state	R_1/Ω	C_1/F	R_2/Ω	C_2/F	R_0/Ω
HRS	107.4	1.55×10^{-10}	1.54×10^5	1.91×10^{-10}	268.3
LRS	356.5	1.74×10^{-10}	/	/	522.9

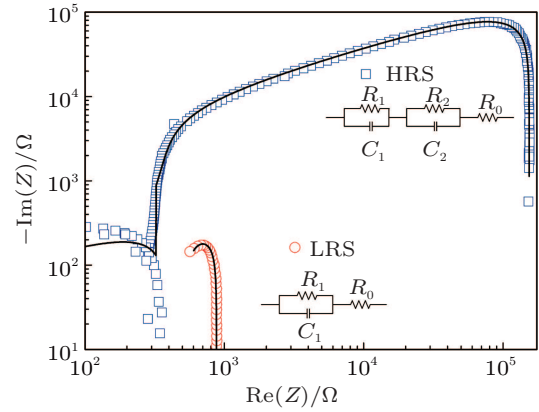


Fig. 4. (color online) Impedance data on log scale in Cole–Cole form in the HRS and LRS with fitting, respectively. Equivalent circuits are shown in the inset. Hollow symbols are experimental data and solid curves are results of fitting.

Mayer discussed the resistive switching characteristics in ferroelectric capacitors and proposed a 2-layer model with a conductive ferroelectric/interfacial dielectric layer sequence to explain the phenomenon.^[45] As discussed before, the contact resistance at the epitaxial BFO/LNO interface is much lower than the one formed at the nonepitaxial Pt/BFO interface, so we consider only the interfacial layer at the Pt/BFZO interface. Based on the Schottky barrier model and considering the multiple steps of resistance change in the conducting filaments model, these two conduction mechanisms may simultaneously exist in our resistive switching device. Such a structure is shown in the schematic diagram in Fig. 5. The movement of oxygen vacancies in BFZO toward the surface has been reported to effectively lower the Schottky barrier height of the Pt top electrode, resulting in large conduction.^[46] With positive voltage applied on the LNO layer, the oxygen vacancies will be pushed to the BFO/Pt interface and accumulate there. Thus, the conductive filaments will be formed. Furthermore, the Schottky barrier height has been effectively decreased. Thus, conductive filaments from LNO to Pt layers without an interfacial Schottky barrier have been formed, and only one semicircle can be observed in the impedance spectra. The device is switched to the LRS. With negative voltage applied on the LNO electrode, the oxygen vacancies will be tracked out from the BFO/Pt interface. The conductive filaments are broken, and the Schottky barrier height is increased. The device switches to the HRS, and rectifying I – V can be observed. Two semi-circles can be observed in the impedance spectra in the HRS. The formation/rupture of the conductive filaments mainly happens at the interface with the top Pt electrodes, which is widely used to explain the mechanism of the unipolar resistive switching (URS).^[47,48] The polarity-dependent resistive switching might be due to the asymmetry of the bottom and top electrodes, and the formation of the Schottky barrier

at the top interface with the Pt electrodes.^[49]

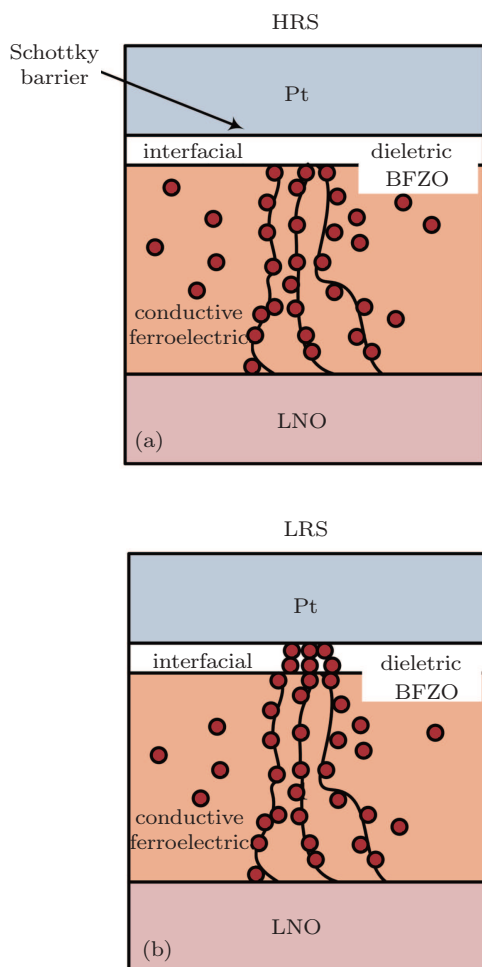


Fig. 5. (color online) Schematic diagrams of resistive switching mechanism: (a) HRS and (b) LRS.

4. Conclusions

In summary, BFZO films have been prepared by pulsed laser deposition on (001) STO substrate with LNO as buffer layer and bottom electrode, and Pt as top electrode. BRS with a resistive ratio of the HRS to the LRS of over three orders of magnitude has been observed. From the I - V characteristics, the conduction of the LRS is dominantly Ohmic, while the HRS is dominated by the SCLC together with Schottky emission at the BFZO/Pt interface. With the impedance spectra, 2-layer structure of conductive ferroelectric/interface dielectric layers has been suggested, and the resistive switching behavior is concluded to be due to the formation/rupture of conductive filaments in the interface dielectric layer close to the top Pt electrodes.

References

- [1] Waser R and Aono M 2007 *Nat. Mater.* **6** 833
- [2] Waser R, Dittmann R, Staikov G and Szot K 2009 *Adv. Mater.* **21** 2632
- [3] Beck A, Bednorz J G, Gerber Ch, Rossel C and Widmer D 2000 *Appl. Phys. Lett.* **77** 139
- [4] Moreno C, Munuera C, Valencia S, Kronast F and Obradors X 2010 *Nano Lett.* **10** 3828
- [5] Yu S, Wu Y and Wong H S Philip 2011 *Appl. Phys. Lett.* **98** 103514
- [6] You Y, So B, Hwang J, Cho W, Lee S S, Chung T, Kim C and An K 2006 *Appl. Phys. Lett.* **89** 222105
- [7] Tsunoda K, Fukuzumi Y, Jameson J R, Wang Z, Griffin P B and Nishi Y 2007 *Appl. Phys. Lett.* **90** 113501
- [8] Seong T, Choi K B, Seo I, Oh J, Moon J W, Hong K and Nahm S 2012 *Appl. Phys. Lett.* **100** 212111
- [9] Mojarad S, Goss J, Kwa K, Zhou Z, Al-Hamadany R S, Appleby D R, Ponon N and O'Neill A 2012 *Appl. Phys. Lett.* **101** 173507
- [10] Kwon D, Kim K M, Jang J H, Jeon J M, Lee M H, Kim G H, Li X, Park G, Lee B, Han S, Kim M and Hwang C S 2010 *Nat. Nanotechnol.* **5** 149
- [11] Magyari-Köpe B, Tendulkar M, Park S, Lee H and Nishi Y 2011 *Nanotechnology* **22** 254029
- [12] Li J, Ohashi N, Okushi H and Haneda H 2011 *Phys. Rev. B* **83** 125317
- [13] Sun J, Jia C H, Li G Q and Zhang W F 2012 *Appl. Phys. Lett.* **101** 133506
- [14] Wang J, Neaton J B, Nagaragan V, Ogale S B, Liu B, Viehland D, Vaithyanathan V, Schlom D G, Waghmare U V, Spaldin N A, Rabe K M, Wuttig M and Ramesh R 2003 *Science* **299** 1719
- [15] Chu Y H, Martin L W, Holcomb M B, Gajek M, Han S J, He Q, Blake N, Yang C H, Lee D, Hu W, Zhan Q, Yang P L, Fraile-Rodriuez A, Scholl A, Wang A X and Ramesh R 2008 *Nat. Mater.* **7** 478
- [16] Yang S Y, Seidel J, Byrnes S J, Shafer P, Yang C H, Rossell M D, Yu P, Chu Y H, Scott J F, Anger J W, Martin L W and Ramesh R 2010 *Nat. Nanotechnol.* **5** 143
- [17] Yang C H, Seidel J, Kim S Y, Rossen P B, Yu P, Gajek M, Chu Y H, Martin L W, Holcomb M B, He Q, Maksymovych P, Balke N, Kalinin S V, Baddorf A P, Basu S R, Scullin M L and Ramesh R 2009 *Nat. Mater.* **8** 485
- [18] Shuai Y, Zhou S, Bürger D, Helm M and Schmidt H 2011 *J. Appl. Phys.* **109** 124117
- [19] Li M, Zhuge F, Zhu X, Yin K, Wang J, Liu Y, He C, Chen B and Li R 2010 *Nanotechnology* **21** 425202
- [20] Yin K, Li M, Liu Y, He C, Zhuge F, Chen B, Lu W, Pan X and Li R 2010 *Appl. Phys. Lett.* **97** 042101
- [21] Wang C, Jin K, Xu Z, Wang L, Ge C, Lu H, Guo H, He M and Yang G 2011 *Appl. Phys. Lett.* **98** 192901
- [22] Hu G D, Fan S H, Yang C H and Wu W B 2008 *Appl. Phys. Lett.* **92** 192905
- [23] Park J M, Gotoda F, Nakashima S, Kanashima T and Okuyama M 2011 *Curr. Appl. Phys.* **11** S270
- [24] Yuan X, Xue X, Zhang X, Wen Z, Yang M, Du J, Wu D and Xu Q 2012 *Solid State Commun.* **152** 241
- [25] Yuan X, Xue X, Si L, Du J and Xu Q 2012 *Chin. Phys. Lett.* **29** 097701
- [26] Zavaliche F, Yang S Y, Zhao T, Chu Y H, Cruz M P, Eom C B and Ramesh R 2006 *Phase Trans.* **79** 991
- [27] Gutiérrez D, Foerster M, Fina I and Fontcuberta J 2012 *Phys. Rev. B* **86** 125309
- [28] Miyazaki H, Goto T, Miwa Y, Ohno T, Suzuki H, Ota T and Takahashi M 2004 *J. Eur. Ceram. Soc.* **24** 1005
- [29] Zhang J, Yang H, Zhang Q, Dong S and Luo J K 2013 *Appl. Phys. Lett.* **102** 012113
- [30] Choi B J, Jeong D S, Kim S K, Rohde C, Choi S, Oh J H, Kim H J, Hwang C S, Szot K, Waser R, Reichenberg B and Tiedke S 2005 *J. Appl. Phys.* **98** 033715
- [31] Kim K M, Choi B J and Hwang C S 2007 *Appl. Phys. Lett.* **90** 242906
- [32] Yang Y C, Pan F, Liu Q, Liu M and Zeng F 2009 *Nano Lett.* **9** 1636
- [33] Liu Q, Dou C, Wang Y, Long S, Wang W, Liu M, Zhang M and Chen J 2009 *Appl. Phys. Lett.* **95** 023501
- [34] Yang T, Harn Y, Chiu K, Fan C and Wu J 2012 *J. Mater. Chem.* **22** 17071
- [35] Yang H, Luo H M, Wang H, Usov I O, Suvorova N A, Jain M, Feldmann D M, Dowden P C, Felmann R F and Jia Q X 2008 *Appl. Phys. Lett.* **92** 102113
- [36] Tsurumaki A, Yamada H and Sawa A 2012 *Adv. Funct. Mater.* **22** 1040
- [37] Pabst G W, Martin L W, Chu Y H and Ramesh R 2007 *Appl. Phys. Lett.* **90** 072902

- [38] Yang H, Jain M, Suvorova N A, Zhou H, Luo H M, Feldmann D M, Dowden P C, De Paula R F, Foltyn S R and Jia Q X 2007 *Appl. Phys. Lett.* **91** 072911
- [39] Xu Q, Yuan X and Xu M 2012 *J. Supercond. Nov. Magn.* **25** 1139
- [40] Ji Z, Mao Q and Ke W 2010 *Solid State Commun.* **150** 1919
- [41] Wang C, Takahashi M, Fujino H, Zhao X, Kume E, Horiuchi T and Sakai S 2006 *J. Appl. Phys.* **99** 054104
- [42] Wen Z, Shen X, Wu J, Wu D, Li A, Yang B, Wang Z, Chen H and Wang J 2010 *Appl. Phys. Lett.* **96** 202904
- [43] Iakovlev S, Solterbeck C H, Kuhnke M and Es-Souni M 2005 *J. Appl. Phys.* **97** 094901
- [44] Schmidt R, Eerenstein W, Winiecki T, Morrison F D and Midgley P A 2007 *Phys. Rev. B* **75** 255111
- [45] Meyer R, Rodriguez Contreras J, Petraru A and Kohlstedt H 2004 *Int. Ferroelectrics* **64** 77
- [46] Farokhipoor S and Noheda B 2012 *J. Appl. Phys.* **112** 052003
- [47] Sawa A 2008 *Mater. Today* **11** 28
- [48] Nagashima K, Yanagida T, Oka K and Kawai T 2009 *Appl. Phys. Lett.* **94** 242902
- [49] Verrelli E, Tsoukalas D, Normand P, Kean A H and Boukos N 2013 *Appl. Phys. Lett.* **102** 022909

JUST FOR AUTHORS
— CHINESE PHYSICS B

Chinese Physics B

Volume 22

Number 10

October 2013

TOPICAL REVIEW — Magnetism, magnetic materials, and interdisciplinary research

104301 Magnetic microbubble: A biomedical platform co-constructed from magnetism and acoustics

Yang Fang, Gu Zhu-Xiao, Jin Xin, Wang Hao-Yao and Gu Ning

107503 Chemical synthesis of magnetic nanocrystals: Recent progress

Liu Fei, Zhu Jing-Han, Hou Yang-Long and Gao Song

108104 Magnetic-mediated hyperthermia for cancer treatment: Research progress and clinical trials

Zhao Ling-Yun, Liu Jia-Yi, Ouyang Wei-Wei, Li Dan-Ye, Li Li, Li Li-Ya and Tang Jin-Tian

RAPID COMMUNICATION

104503 Noether symmetry and conserved quantities of the analytical dynamics of a Cosserat thin elastic rod

Wang Peng, Xue Yun and Liu Yu-Lu

106804 Resonant energy transfer from nanocrystal Si to β -FeSi₂ in hybrid Si/ β -FeSi₂ film

He Jiu-Yang, Zhang Qi-Zhen, Wu Xing-Long and Chu Paul K.

107801 The design and preparation of a Fabry–Pérot polarizing filter

Hou Yong-Qiang, Qi Hong-Ji and Yi Kui

GENERAL

100201 A diagrammatic categorification of the fermion algebra

Lin Bing-Sheng, Wang Zhi-Xi, Wu Ke and Yang Zi-Feng

100202 Approximate derivative-dependent functional variable separation for quasi-linear diffusion equations with a weak source

Ji Fei-Yu and Yang Chun-Xiao

100203 On certain new exact solutions of the Einstein equations for axisymmetric rotating fields

Lakhveer Kaur and R. K. Gupta

100204 An element-free Galerkin (EFG) method for numerical solution of the coupled Schrödinger-KdV equations

Liu Yong-Qing, Cheng Rong-Jun and Ge Hong-Xia

100301 A geometric phase for superconducting qubits under the decoherence effect

S. Abdel-Khalek, K. Berrada, Mohamed A. El-Sayed and M. Abel-Aty

100302 Analytic solutions of the double ring-shaped Coulomb potential in quantum mechanics

Chen Chang-Yuan, Lu Fa-Lin, Sun Dong-Sheng and Dong Shi-Hai

100303 Relativistic treatment of the spin-zero particles subject to the second Pöschl–Teller-like potential

Ekele V. Aguda and Amos S. Idowu

100304 The spin-one Duffin–Kemmer–Petiau equation in the presence of pseudo-harmonic oscillatory ring-shaped potential

H. Hassanabadi and M. Kamali

(Continued on the Bookbinding Inside Back Cover)

- 100305 Eigen-spectra in the Dirac-attractive radial problem plus a tensor interaction under pseudospin and spin symmetry with the SUSY approach**
S. Arbab Moghadam, H. Mehraban and M. Eshghi
- 100306 Quantum correlation of a three-particle W -class state under quantum decoherence**
Xu Peng, Wang Dong and Ye Liu
- 100307 Enhanced electron–positron pair creation by the frequency chirped laser pulse**
Jiang Min, Xie Bai-Song, Sang Hai-Bo and Li Zi-Liang
- 100308 Generation of steady four-atom decoherence-free states via quantum-jump-based feedback**
Wu Qi-Cheng and Ji Xin
- 100309 Bound entanglement and teleportation for arbitrary bipartite systems**
Fan Jiao and Zhao Hui
- 100501 Transport dynamics of an interacting binary Bose–Einstein condensate in an incommensurate optical lattice**
Cui Guo-Dong, Sun Jian-Fang, Jiang Bo-Nan, Qian Jun and Wang Yu-Zhu
- 100502 Reliability of linear coupling synchronization of hyperchaotic systems with unknown parameters**
Li Fan, Wang Chun-Ni and Ma Jun
- 100503 Synchronization for complex dynamical Lurie networks**
Zhang Xiao-Jiao and Cui Bao-Tong
- 100504 Robust modified projective synchronization of fractional-order chaotic systems with parameters perturbation and external disturbance**
Wang Dong-Feng, Zhang Jin-Ying and Wang Xiao-Yan
- 100505 Four-cluster chimera state in non-locally coupled phase oscillator systems with an external potential**
Zhu Yun, Zheng Zhi-Gang and Yang Jun-Zhong
- 100506 Chaos synchronization of a chain network based on a sliding mode control**
Liu Shuang and Chen Li-Qun
- 100507 Trial function method and exact solutions to the generalized nonlinear Schrödinger equation with time-dependent coefficient**
Cao Rui and Zhang Jian
- 100508 Phase diagrams of spin-3/2 Ising model in the presence of random crystal field within the effective field theory based on two approximations**
Ali Yigit and Erhan Albayrak
- 100701 MEH-PPV/Alq₃-based bulk heterojunction photodetector**
Zubair Ahmad, Mahdi Hasan Suhail, Issam Ibrahim Muhammad, Wissam Khayer Al-Rawi, Khaulah Sulaiman, Qayyum Zafar, Ahmad Sazali Hamzah and Zurina Shaameri
- 100702 Multi-rate sensor fusion-based adaptive discrete finite-time synergetic control for flexible-joint mechanical systems**
Xue Guang-Yue, Ren Xue-Mei and Xia Yuan-Qing
- 100703 Analysis of influence of RF power and buffer gas pressure on sensitivity of optically pumped cesium magnetometer**
Shi Rong-Ye and Wang Yan-Hui

(Continued on the Bookbinding Inside Back Cover)

ATOMIC AND MOLECULAR PHYSICS

- 103101** Translational, vibrational, rotational enhancements and alignments of reactions $\text{H} + \text{ClF} (v = 0-5, j = 0, 3, 6, 9) \rightarrow \text{HCl} + \text{F}$ and $\text{HF} + \text{Cl}$, at $E_{\text{rel}} = 0.5-20$ kcal/mol
Victor Wei-Keh Chao(Wu)
- 103102** Further investigations of the low-lying electronic states of AsO^+ radical
Zhu Zun-Lue, Qiao Hao, Lang Jian-Hua and Sun Jin-Feng
- 103103** Time-dependent density functional theoretical studies on the photo-induced dynamics of an HCl molecule encapsulated in C_{60} under femtosecond laser pulses
Liu Dan-Dan and Zhang Hong
- 103301** Control of the photoionization/photodissociation processes of cyclopentanone with trains of femtosecond laser pulses
Song Yao-Dong, Chen Zhou, Yang Xue, Sun Chang-Kai, Zhang Cong-Cong and Hu Zhan
- 103401** The effect of wave function orthogonality on the simultaneous ionization and excitation of helium
Liu Li-Juan, Jia Chang-Chun, Zhang Li-Min, Chen Jiao-Jiao and Chen Zhang-Jin
- 103402** Multiple ionization of atoms and molecules impacted by very high- q fast projectiles in the strong coupling regime ($q/v > 1$)
Zhou Man, Zou Xian-Rong, Zhao Lei, Chen Xi-Meng, Wang Shi-Yao, Zhou Wang and Shao Jian-Xiong
- 103403** Kr L X-ray and Au M X-ray emission for 1.5 MeV–3.9 MeV Kr^{13+} ions impacting on an Au target
Mei Ce-Xiang, Zhang Xiao-An, Zhao Yong-Tao, Zhou Xian-Ming, Ren Jie-Ru, Wang Xing, Lei Yu, Sun Yuan-Bo, Cheng Rui, Wang Yu-Yu, Liang Chang-Hui, Li Yao-Zong and Xiao Guo-Qing
- 103701** Experiments on trapping ytterbium atoms in optical lattices
Zhou Min, Chen Ning, Zhang Xiao-Hang, Huang Liang-Yu, Yao Mao-Fei, Tian Jie, Gao Qi, Jiang Hai-Ling, Tang Hai-Yao and Xu Xin-Ye

ELECTROMAGNETISM, OPTICS, ACOUSTICS, HEAT TRANSFER, CLASSICAL MECHANICS, AND FLUID DYNAMICS

- 104101** Flat lenses constructed by graded negative index-based photonic crystals with tuned configurations
Jin Lei, Zhu Qing-Yi, Fu Yong-Qi and Yu Wei-Xing
- 104201** The Wigner distribution function of a super Lorentz–Gauss SLG_{11} beam through a paraxial $ABCD$ optical system
Zhou Yi-Min and Zhou Guo-Quan
- 104202** An improved deconvolution method for X-ray coded imaging in inertial confinement fusion
Zhao Zong-Qing, He Wei-Hua, Wang Jian, Hao Yi-Dan, Cao Lei-Feng, Gu Yu-Qiu and Zhang Bao-Han
- 104203** Phase grating in a doubly degenerate four-level system
Liu Yun, Wang Pu and Peng Shuang-Yan
- 104204** Curved surface effect and emission on silicon nanostructures
Huang Wei-Qi, Yin Jun, Zhou Nian-Jie, Huang Zhong-Mei, Miao Xin-Jian, Cheng Han-Qiong, Su Qin, Liu Shi-Rong and Qin Chao-Jian
- 104205** An all-polarization-maintaining repetition-tunable erbium-doped passively mode-locked fiber laser
Zhao Guang-Zhen, Xiao Xiao-Sheng, Meng Fei, Mei Jia-Wei and Yang Chang-Xi

- 104206 A mode-locked external-cavity quantum-dot laser with a variable repetition rate**
Wu Jian, Jin Peng, Li Xin-Kun, Wei Heng, Wu Yan-Hua, Wang Fei-Fei, Chen Hong-Mei, Wu Ju and Wang Zhan-Guo
- 104207 The dependence on optical energy of terahertz emission from air plasma induced by two-color femtosecond laser-pulses**
Wu Si-Qing, Liu Jin-Song, Wang Sheng-Lie and Hu Bing
- 104208 Optical bistability induced by quantum coherence in a negative index atomic medium**
Zhang Hong-Jun, Guo Hong-Ju, Sun Hui, Li Jin-Ping and Yin Bao-Yin
- 104209 The mobility of nonlocal solitons in fading optical lattices**
Dai Zhi-Ping, Ling Xiao-Hui, Wang You-Wen and You Kai-Ming
- 104210 The influence of smoothing by spectral dispersion on the beam characteristics in the near field**
Fan Xin-Min, Lü Zhi-Wei, Lin Dian-Yang and Wang Yu-Lei
- 104211 Characteristics of photonic bands generated by quadrangular multiconnected networks**
Luo Rui-Fang, Yang Xiang-Bo, Lu Jian and Liu Timon Cheng-Yi
- 104212 Optical phase front control in a metallic grating with equally spaced alternately tapered slits**
Zheng Gai-Ge, Wu Yi-Gen and Xu Lin-Hua
- 104213 A high figure of merit localized surface plasmon sensor based on a gold nanograting on the top of a gold planar film**
Zhang Zu-Yin, Wang Li-Na, Hu Hai-Feng, Li Kang-Wen, Ma Xun-Peng and Song Guo-Feng
- 104501 A necessary and sufficient condition for transforming autonomous systems into linear autonomous Birkhoffian systems**
Cui Jin-Chao, Liu Shi-Xing and Song Duan
- 104502 The dynamic characteristics of harvesting energy from mechanical vibration via piezoelectric conversion**
Fan Kang-Qi, Ming Zheng-Feng, Xu Chun-Hui and Chao Feng-Bo
- 104701 Electro-magnetic control of shear flow over a cylinder for drag reduction and lift enhancement**
Zhang Hui, Fan Bao-Chun, Chen Zhi-Hua, Chen Shuai and Li Hong-Zhi

PHYSICS OF GASES, PLASMAS, AND ELECTRIC DISCHARGES

- 105101 The mechanism of hydrogen plasma passivation for poly-crystalline silicon thin film**
Li Juan, Luo Chong, Meng Zhi-Guo, Xiong Shao-Zhen and Hoi Sing Kwok

CONDENSED MATTER: STRUCTURAL, MECHANICAL, AND THERMAL PROPERTIES

- 106101 Silicon micro-hemispheres with periodic nanoscale rings produced by the laser ablation of single crystalline silicon**
Chen Ming, Li Shuang, Cui Qing-Qiang and Liu Xiang-Dong
- 106102 TiO₂/Ag composite nanowires for a recyclable surface enhanced Raman scattering substrate**
Deng Chao-Yue, Zhang Gu-Ling, Zou Bin, Shi Hong-Long, Liang Yu-Jie, Li Yong-Chao, Fu Jin-Xiang and Wang Wen-Zhong
- 106103 A phase-field model for simulating various spherulite morphologies of semi-crystalline polymers**
Wang Xiao-Dong, Ouyang Jie, Su Jin and Zhou Wen

- 106104 Effect of vacancy charge state on positron annihilation in silicon**
Liu Jian-Dang, Cheng Bin, Kong Wei and Ye Bang-Jiao
- 106105 Optical and magnetic properties of InFeP layers prepared by Fe⁺ implantation**
Zhou Lin, Shang Yan-Xia, Wang Ze-Song, Zhang Rui, Zhang Zao-Di, Vasiliy O. Pelenovich, Fu De-Jun and Kang Tae Won
- 106106 Effect of In_xGa_{1-x}N “continuously graded” buffer layer on InGaN epilayer grown by metalorganic chemical vapor deposition**
Qian Wei-Ning, Su Shi-Chen, Chen Hong, Ma Zi-Guang, Zhu Ke-Bao, He Miao, Lu Ping-Yuan, Wang Geng, Lu Tai-Ping, Du Chun-Hua, Wang Qiao, Wu Wen-Bo and Zhang Wei-Wei
- 106107 Electric field modulation technique for high-voltage AlGaIn/GaN Schottky barrier diodes**
Tang Cen, Xie Gang, Zhang Li, Guo Qing, Wang Tao and Sheng Kuang
- 106108 Accurate measurement and influence on device reliability of defect density of a light-emitting diode**
Guo Zu-Qiang and Qian Ke-Yuan
- 106109 Effects of chromium on structure and mechanical properties of vanadium: A first-principles study**
Gui Li-Jiang, Liu Yue-Lin, Wang Wei-Tian, Zhang Ying, Lü Guang-Hong and Yao Jun-En
- 106201 Size effect of the elastic modulus of rectangular nanobeams: Surface elasticity effect**
Yao Hai-Yan, Yun Guo-Hong and Fan Wen-Liang
- 106401 Thermodynamic properties of 3C–SiC**
B. Y. Thakore, S. G. Khambholja, A. Y. Vahora, N. K. Bhatt and A. R. Jani
- 106801 Fabrication of pillar-array superhydrophobic silicon surface and thermodynamic analysis on the wetting state transition**
Liu Si-Si, Zhang Chao-Hui, Zhang Han-Bing, Zhou Jie, He Jian-Guo and Yin Heng-Yang
- 106802 Fabrication of GaN-based LEDs with 22° undercut sidewalls by inductively coupled plasma reactive ion etching**
Wang Bo, Su Shi-Chen, He Miao, Chen Hong, Wu Wen-Bo, Zhang Wei-Wei, Wang Qiao, Chen Yu-Long, Gao You, Zhang Li, Zhu Ke-Bao and Lei Yan
- 106803 Influence of Si doping on the structural and optical properties of InGaIn epilayers**
Lu Ping-Yuan, Ma Zi-Guang, Su Shi-Chen, Zhang Li, Chen Hong, Jia Hai-Qiang, Jiang Yang, Qian Wei-Ning, Wang Geng, Lu Tai-Ping and He Miao
- CONDENSED MATTER: ELECTRONIC STRUCTURE, ELECTRICAL, MAGNETIC, AND OPTICAL PROPERTIES**
- 107101 Growth of monodisperse nanospheres of MnFe₂O₄ with enhanced magnetic and optical properties**
M. Yasir Rafique, Pan Li-Qing, Qurat-ul-ain Javed, M. Zubair Iqbal, Qiu Hong-Mei, M. Hassan Farooq, Guo Zhen-Gang and M. Tanveer
- 107102 First-principles calculations of electronic and magnetic properties of CeN: The LDA + *U* method**
Hao Ai-Min and Bai Jing
- 107103 Theoretical optoelectronic analysis of intermediate-band photovoltaic material based on ZnY_{1-x}O_x (Y = S, Se, Te) semiconductors by first-principles calculations**
Wu Kong-Ping, Gu Shu-Lin, Ye Jian-Dong, Tang Kun, Zhu Shun-Ming, Zhou Meng-Ran, Huang You-Rui, Zhang Rong and Zheng You-Dou

(Continued on the Bookbinding Inside Back Cover)

- 107104 The effects of strain and surface roughness scattering on the quasi-ballistic characteristics of a Ge nanowire p-channel field-effect transistor**
Qin Jie-Yu, Du Gang and Liu Xiao-Yan
- 107105 The structural, elastic, and electronic properties of $Zr_xNb_{1-x}C$ alloys from first principle calculations**
Sun Xiao-Wei, Zhang Xin-Yu, Zhang Su-Hong, Zhu Yan, Wang Li-Min, Zhang Shi-Liang, Ma Ming-Zhen and Liu Ri-Ping
- 107106 The nonlinear optical properties of a magneto-exciton in a strained $Ga_{0.2}In_{0.8}As/GaAs$ quantum dot**
N. R. Senthil Kumar, A. John Peter and Chang Kyoo Yoo
- 107201 Structural and electrical properties of laser-crystallized nanocrystalline Ge films and nanocrystalline Ge/SiN_x multilayers**
Li Cong, Xu Jun, Li Wei, Jiang Xiao-Fan, Sun Sheng-Hua, Xu Ling and Chen Kun-Ji
- 107202 A shortcut for determining growth mode**
R. A. Rehman, Cai Yi-Liang, Zhang Han-Jie, Wu Ke, Dou Wei-Dong, Li Hai-Yang, He Pi-Mo and Bao Shi-Ning
- 107301 Temperature-dependent rectifying and photovoltaic characteristics of an oxygen-deficient $Bi_2Sr_2Co_2O_y/Si$ heterojunction**
Yan Guo-Ying, Bai Zi-Long, Li Hui-Ling, Fu Guang-Sheng, Liu Fu-Qiang, Yu Wei, Wang Jiang-Long and Wang Shu-Fang
- 107302 High-mobility germanium p-MOSFETs by using HCl and $(NH_4)_2S$ surface passivation**
Xue Bai-Qing, Wang Sheng-Kai, Han Le, Chang Hu-Dong, Sun Bing, Zhao Wei and Liu Hong-Gang
- 107303 The degradation mechanism of an AlGaIn/GaN high electron mobility transistor under step-stress**
Chen Wei-Wei, Ma Xiao-Hua, Hou Bin, Zhu Jie-Jie, Zhang Jin-Cheng and Hao Yue
- 107401 A new modulated structure in α -Fe₂O₃ nanowires**
Cai Rong-Sheng, Shang Lei, Liu Xue-Hua, Wang Yi-Qian, Yuan Lu and Zhou Guang-Wen
- 107501 The variation of Mn-dopant distribution state with x and its effect on the magnetic coupling mechanism in $Zn_{1-x}Mn_xO$ nanocrystals**
Cheng Yan, Hao Wei-Chang, Li Wen-Xian, Xu Huai-Zhe, Chen Rui and Dou Shi-Xue
- 107502 Transformation behaviors, structural and magnetic characteristics of Ni–Mn–Ga films on MgO (001)**
Xie Ren, Tang Shao-Long, Tang Yan-Mei, Liu Xiao-Chen, Tang Tao and Du You-Wei
- 107701 Dielectric spectroscopy studies of ZnO single crystal**
Cheng Peng-Fei, Li Sheng-Tao and Wang Hui
- 107702 Bipolar resistive switching in $BiFe_{0.95}Zn_{0.05}O_3$ films**
Yuan Xue-Yong, Luo Li-Rong, Wu Di and Xu Qing-Yu
- 107703 Analysis of tensile strain enhancement in Ge nano-belts on an insulator surrounded by dielectrics**
Lu Wei-Fang, Li Cheng, Huang Shi-Hao, Lin Guang-Yang, Wang Chen, Yan Guang-Ming, Huang Wei, Lai Hong-Kai and Chen Song-Yan
- 107802 The effect of an optical pump on the absorption coefficient of magnesium-doped near-stoichiometric lithium niobate in terahertz range**
Zuo Zhi-Gao, Ling Fu-Ri, Ma De-Cai, Wu Liang, Liu Jin-Song and Yao Jian-Quan

(Continued on the Bookbinding Inside Back Cover)

- 107803** *In-situ* growth of a CdS window layer by vacuum thermal evaporation for CIGS thin film solar cell applications
Cao Min, Men Chuan-Ling, Zhu De-Ming, Tian Zi-Ao and An Zheng-Hua
- 107804** The metamaterial analogue of electromagnetically induced transparency by dual-mode excitation of a symmetric resonator
Shao Jian, Li Jie, Li Jia-Qi, Wang Yu-Kun, Dong Zheng-Gao, Lu Wei-Bing and Zhai Ya
- 107805** Tunable zeroth-order resonator based on a ferrite metamaterial structure
Javad Ghalibafan and Nader Komjani
- 107806** Structural distortions and magnetisms in Fe-doped $\text{LaMn}_{1-x}\text{Fe}_x\text{O}_3$ ($0 < x \leq 0.6$)
Zheng Long and Wu Xiao-Shan
- 107901** A comparison of the field emission characteristics of vertically aligned graphene sheets grown on different SiC substrates
Chen Lian-Lian, Guo Li-Wei, Liu Yu, Li Zhi-Lin, Huang Jiao and Lu Wei
- INTERDISCIPLINARY PHYSICS AND RELATED AREAS OF SCIENCE AND TECHNOLOGY**
- 108101** Controllable synthesis, characterization, and growth mechanism of hollow $\text{Zn}_x\text{Cd}_{1-x}\text{S}$ spheres generated by a one-step thermal evaporation method
Yang Zai-Xing, Zhong Wei, Au Chak-Tong and Du You-Wei
- 108102** The effect of fractional thermoelasticity on a two-dimensional problem of a mode I crack in a rotating fiber-reinforced thermoelastic medium
Ahmed E. Abouelregal and Ashraf M. Zenkour
- 108103** Crystal growth, structural and physical properties of the 5d noncentrosymmetric LaOsSi_3
Zhang Xu, Miao Shan-Shan, Wang Pu, Zheng Ping, Yin Wen-Long, Yao Ji-Yong, Jiang Hong-Wei, Wang Hai and Shi You-Guo
- 108301** A fiber-array probe technique for measuring the viscosity of a substance under shock compression
Feng Li-Peng, Liu Fu-Sheng, Ma Xiao-Juan, Zhao Bei-Jing, Zhang Ning-Chao, Wang Wen-Peng and Hao Bin-Bin
- 108401** A novel slotted helix slow-wave structure for high power Ka-band traveling-wave tubes
Liu Lu-Wei, Wei Yan-Yu, Wang Shao-Meng, Hou Yan, Yin Hai-Rong, Zhao Guo-Qing, Duan Zhao-Yun, Xu Jin, Gong Yu-Bin, Wang Wen-Xiang and Yang Ming-Hua
- 108402** The design and numerical analysis of tandem thermophotovoltaic cells
Yang Hao-Yu, Liu Ren-Jun, Wang Lian-Kai, Lü You, Li Tian-Tian, Li Guo-Xing, Zhang Yuan-Tao and Zhang Bao-Lin
- 108501** Gate-to-body tunneling current model for silicon-on-insulator MOSFETs
Wu Qing-Qing, Chen Jing, Luo Jie-Xin, Lü Kai, Yu Tao, Chai Zhan and Wang Xi
- 108502** Analyses of temperature-dependent interface states, series resistances, and AC electrical conductivities of Al/p-Si and $\text{Al/Bi}_4\text{Ti}_3\text{O}_{12}/\text{p-Si}$ structures by using the admittance spectroscopy method
Mert Yıldırım, Perihan Durmuş, and Şemsettin Altındal
- 108503** Design and fabrication of a high-performance evanescently coupled waveguide photodetector
Liu Shao-Qing, Yang Xiao-Hong, Liu Yu, Li Bin and Han Qin

(Continued on the Bookbinding Inside Back Cover)

108504 Preliminary results for the design, fabrication, and performance of a backside-illuminated avalanche drift detector

Qiao Yun, Liang Kun, Chen Wen-Fei and Han De-Jun

108505 Performance enhancement of an InGaN light-emitting diode with an AlGaN/InGaN superlattice electron-blocking layer

Xiong Jian-Yong, Xu Yi-Qin, Zhao Fang, Song Jing-Jing, Ding Bin-Bin, Zheng Shu-Wen, Zhang Tao and Fan Guang-Han

108901 A comparison of coal supply-demand in China and in the US based on a network model

Fang Cui-Cui, Sun Mei, Zhang Pei-Pei and Gao An-Na

108902 The effect of moving bottlenecks on a two-lane traffic flow

Fang Yuan, Chen Jian-Zhong and Peng Zhi-Yuan

108903 An improvement of the fast uncovering community algorithm

Wang Li, Wang Jiang, Shen Hua-Wei and Cheng Xue-Qi

108904 Random walks in generalized delayed recursive trees

Sun Wei-Gang, Zhang Jing-Yuan and Chen Guan-Rong

GEOPHYSICS, ASTRONOMY, AND ASTROPHYSICS

109501 Modeling and assessing the influence of linear energy transfer on multiple bit upset susceptibility

Geng Chao, Liu Jie, Xi Kai, Zhang Zhan-Gang, Gu Song and Liu Tian-Qi

JUST FOR AUTHORS
— CHINESE PHYSICS B